MULTICYCLIC JET-FLAP CONTROL FOR ALLEVIATION OF HELICOPTER BLADE STRESSES AND FUSELAGE VIBRATION

John L. McCloud, III* and Marcel Kretz**
Ames Research Center, Moffett Field, California 94035

Abstract

Results of wind tunnel tests of a 12-meter-diameter rotor utilizing multicyclic jet-flap control deflection are presented. Analyses of these results are shown, and experimental transfer functions are determined by which optimal control vectors are developed. These vectors are calculated to eliminate specific harmonic bending stresses, minimize rms levels (a measure of the peak-to-peak stresses), or minimize vertical vibratory loads that would be transmitted to the fuselage.

Although the specific results and the ideal control vectors presented are for a specific jet-flap driven rotor, the method employed for the analyses is applicable to similar investigations. A discussion of possible alternative methods of multicyclic control by mechanical flaps or nonpropulsive jet-flaps is presented.

Notation

a, b, c, ...	matrix elements
b	number of blades
c	chord of blades
c_l	blade section lift coefficient
Δc_l	increment of blade section lift coefficient due to multicyclic jet-flap deflection
$\bar{C}_L$	rotor average lift coefficient $(6C_{LR}/\sigma)$
C_{LR}/σ	rotor lift coefficient $(L/\rho(\Omega R)^2 bcR)$
C_{XR}/σ	rotor propulsive force coefficient $(X/\rho(\Omega R)^2 bcR)$
C_{YR}/σ	rotor side-force coefficient $(Y/\rho(\Omega R)^2 bcR)$
F_1, F_2, F_3	forces measured below the rotor hub
L	rotor lift
R	rotor radius
T	transfer matrix
V	forward flight velocity
V_{n_c}	cosine component of the summation of forces F for the nth harmonic
V_{n_s}	sine component of the summation of forces F for the nth harmonic
X	rotor propulsive force
Y	rotor side force
α_s	rotor shaft axis inclination
δ	jet-flap deflection angle
$\theta_{3P} = \frac{1}{3}\tan^{-1}(\delta_{3s}/\delta_{3c})$ $\theta_{4P} = \frac{1}{4}\tan^{-1}(\delta_{4s}/\delta_{4c})$	azimuth angles for maximum deflection
σ	blade bending stress (or rotor solidity for rotor coefficient definitions)
ρ	air density
ψ	azimuth position
Ω	rotor rotational velocity

Subscripts

c	cosine
m	variable parts
p	primary control
s	sine
0, 1, 2, 3 . . .n	harmonic number

Superscript

T	transpose of matrix or vector

(Units are as noted, or such as to produce unitless coefficients.)

Introduction

To achieve its full potential as the most effective VTOL aircraft, the helicopter must drastically reduce its characteristic vibrations and attendant high maintenance costs. As shown in Reference 1, helicopter maintenance costs are twice those of fixed-wing aircraft of the same empty weight. With the same basic elements — engines, gear boxes, pumps, propellers, and avionics equipment — in both aircraft, this difference is assuredly traceable to the high vibration environment of helicopter components. Coping with this environment, helicopter designers are forced to provide heavier systems, which result in higher ratios of empty weight to payload. These ratios combine to yield maintenance costs per unit payload that are greater than twice those of fixed-wing aircraft. The relationship between oscillating loads — hence vibration — and maintenance costs has been dramatically demonstrated and reported in Reference 2. As shown in that report, the Sikorsky bifilar system reduced rotor-induced vibratory loads by 54.3%, which in turn reduced failure rates so that 48% fewer replacement parts were required, and overall maintenance costs were reduced by 38.5%.

Many vibration suppression systems are being investigated by various groups. These systems are characterized as either absorption, isolation, or active control. The multicyclic jet-flap control is an active control system, which controls or modulates the oscillating loads at their source, that is, on the blades themselves. That we can effectively change the loading distribution of a helicopter rotor in forward flight so as to reduce cyclic blade stress variations, or to reduce vibratory loads transmitted to the fuselage, has been demonstrated by large-scale wind tunnel tests of the Giravions Dorand jet-flap rotor at Ames Research Center. The rotor, its design, and performance characteristics have been reported on in References 3 and 4. Its supporting wind tunnel test equipment and some of the results of the multicyclic load alleviation tests were presented in Reference 5. Some of that multicyclic test data will be shown herein also.

*Research Scientist
Ames Research Center, Moffett Field, Calif. 94035

**Chief Engineer
Giravions Dorand, 92150 Suresnes, France

The main purpose of this paper is to show the method used to analyze the multivariable data, and how it is possible to develop several "ideal" control schedules or vectors to achieve specific blade stress and vibratory load reductions. A simplified analysis of the results is presented, indicating that multicyclic systems that do not employ propulsive jet-flaps may be feasible.

Rotor and Test Apparatus

The Dorand Rotor is two-bladed, with a teetering hub and offset blade coning hinges, but no feathering hinges. The rotor is driven in rotation by a jet-flap, of the blown mechanical flap type, on the outer 30% of the blade radius. The mechanical flaps are deflected by a swash-plate and cam system, which provided both collective and harmonic control. Swash-plate tilt provided the longitudinal and lateral control, whereas the cams introduced second, third and fourth harmonic variations. The rotor is shown, mounted in the NASA-Ames 40- by 80-ft wind tunnel, in Figure 1. Further details of the rotor and test apparatus are given in References 3, 4, 5, and 6.

Results and Analysis

The wind tunnel tests, their range and the modi operandi, are described in Reference 6. The tests simulated forward flight conditions at blade-loading coefficients C_{LR}/σ somewhat greater than conventional rotors employ.

Figures 2 and 3 (taken from Reference 5) show some typical results from the multicyclic tests. Figure 2 shows three sets of jet-flap deflection angle and blade-bending stresses with and without multicyclic control. Some control distortion is affecting the "without multicyclic control" in that the deflection is not purely sinusoidal. The basic bending stresses are predominantly three per revolution (3P), typical for a relatively stiff, heavy blade. The peak-to-peak stress reductions are 29, 21, and 36%. Figure 3 shows the effect of the multicyclic control on the forces below the hub in the nonrotating system: on the left, traces for three vertical force transducers for the condition of zero multicyclic control; on the right, traces for the same transducers for multicyclic control applied.

These tests produced data for a large number of flight conditions and multicyclic deflection combinations. More of these data are presented in Reference 6, which includes both time histories and harmonic coefficients of blade-bending stress, vertical forces, and jet-flap deflection.

Blade-Bending Stresses

As discussed in Reference 5, the relationships between the time histories of jet-flap deflections and the resulting blade-bending stresses can be expressed by a transfer matrix.* The time histories of jet-flap deflection and blade-bending stress are both expressed as harmonic series. If the harmonic coefficients of the stress variation (Eq. 1) are related to the jet-flap deflection harmonic coefficients (Eq. 2), as shown in Eq. 3, they can be expressed in the matrix form as in Eq. 4.

$$\sigma = \sigma_0 + \sigma_{1_c} \cos\psi + \sigma_{1_s} \sin\psi + \sigma_{2_c} \cos 2\psi + \sigma_{2_s} \sin 2\psi + \cdots \quad (1)$$

$$\delta = \delta_0 + \delta_{1_c} \cos\psi + \delta_{1_s} \sin\psi + \delta_{2_c} \cos 2\psi + \delta_{2_s} \sin 2\psi + \cdots \quad (2)$$

if

$$\sigma_{n_s} = (a_{n_s})(\delta_0) + (b_{n_s})(\delta_{1_c}) + (c_{n_s})(\delta_{1_s}) + (d_{n_s})(\delta_{2_c}) + \cdots (\sigma_{n_{s_0}}) \quad (3)$$

then

$$\begin{vmatrix} \sigma_0 \\ \sigma_{1_c} \\ \sigma_{1_s} \\ \cdot \\ \cdot \\ \sigma_{n_s} \end{vmatrix} = \begin{vmatrix} a_0 & b_0 & c_0 & d_0 & \cdot & \cdot & \sigma_{0_0} \\ a_{1_c} & b_{1_c} & c_{1_c} & d_{1_c} & \cdot & \cdot & \sigma_{1_{c_0}} \\ a_{1_s} & b_{1_s} & c_{1_s} & d_{1_s} & \cdot & \cdot & \sigma_{1_{s_0}} \\ \cdot & \cdot & \cdot & \cdot & \cdot & \cdot & \cdot \\ \cdot & \cdot & \cdot & \cdot & \cdot & \cdot & \cdot \\ a_{n_s} & b_{n_s} & c_{n_s} & d_{n_s} & \cdot & \cdot & \sigma_{n_{s_0}} \end{vmatrix} \times \begin{vmatrix} \delta_0 \\ \delta_{1_c} \\ \delta_{1_s} \\ \cdot \\ \cdot \\ \delta_{n_s} \\ 1 \end{vmatrix} \quad (4)$$

The last term of Eq. 3 and the last column of the transfer matrix represent the harmonics of stress, which are due to the flight condition. With the column matrices or vectors of the harmonic contents of jet-flap deflection and blade stresses known for several conditions, computer routines can solve for the transfer matrix elements.

A sample result of this method was shown in Reference 5, together with correlation plots showing very good agreement between stresses calculated using the transfer matrix and measured stresses. The matrix, based on 15 flight conditions, showed large amounts of interharmonic coupling, particularly for the third and fourth harmonics of stress.

It is apparent from Eq. 4 that it is possible to determine multicyclic jet-flap deflection amplitudes that will eliminate the corresponding higher harmonic stress coefficients. These higher harmonic stress terms are set to zero and the equation is then solved for the required jet-flap deflection coefficients. These coefficients will be hereinafter called the "ideal harmonic control vector." Reference 6 presents some of these control vectors.

Although the objective of zero higher harmonic stresses was achieved, the requisite multicyclic jet-flap deflections produced different amounts of 1P stresses and, in some instances, the peak-to-peak stresses were increased. The changes in 1P stresses imply a change in the rotor's thrust and inplane forces. (Note that the ideal harmonic control vector as determined in Eq. 4 may be considered to be for "fixed stick" conditions as existed in the wind tunnel tests.) Therefore, a second transfer matrix (Eq. 5) was defined as shown below.

*This method of analysis was first suggested and developed by Dr. Jean-Noel Aubrun of Giravions Dorand.

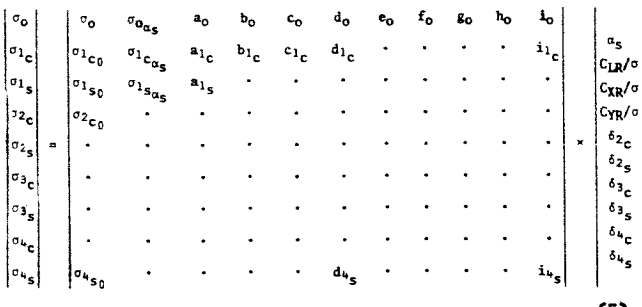

(5)

Notice that the columns of the transfer matrix and the elements of the control vector have been rearranged. The first column represents stress levels for the condition of zero rotor shaft inclination, zero rotor force coefficients, and no jet-flap deflections. The second through fourth columns represent the changes in stress level due to rotor angle of attack and the rotor's force coefficients. The remaining columns correspond to stress derivatives with respect to the multicyclic jet-flap deflections. The control vector has been realigned to reflect the column changes. Note that the matrix elements are no longer defined by Eq. 3, but by Eq. 5 itself, and the basic "collective" and "1P cyclic" terms have now been replaced by the rotor's force coefficients, C_{LR}/σ, C_{XR}/σ and C_{YR}/σ (multiplied by 10^3 for numerical convenience). This can be considered the transfer matrix for "fixed flight" conditions. Correlations for this matrix are not as good as those for the "fixed stick" conditions, probably because of the greater scatter in the force data. However, for 30 test conditions, the correlation is very good, comparable to the 15-test condition correlation shown in Reference 5.

The matrix, based on 30 flight conditions, is shown in Figure 4. Again, it is possible to determine multicyclic jet-flap deflections to produce zero higher harmonic stresses. These deflections also define an ideal harmonic control vector, this time for fixed flight conditions. Although the 1P stresses may still change, and the peak-to-peak stress increase, the rotor's force output is unchanged, at least to the accuracy of the basic methodology.

While elimination of a particular harmonic, or all higher harmonics of stress, may be beneficial, it may be more desirable to reduce other stress parameters, such as the root-mean-square, or the peak-to-peak values. It is difficult to relate peak-to-peak values to the harmonic coefficients, and the iterative algorithm necessary to affect peak-to-peak minimization would be considerably more complex, for example, than one to minimize the root-mean-square values. The rms value of the variable portion of the stresses will be minimized when the sum of the squares of the harmonic coefficients is also minimized. This sum is given by

$$\sigma_m{}^T\sigma_m = \sum_1^4 \left(\sigma_{n_c}{}^2 + \sigma_{n_s}{}^2\right) \qquad (6)$$

This product will be minimized when the multicyclic deflections are given by

$$\delta_{irms} = -(T_m{}^T T_m)^{-1}(T_m{}^T T_p)\ \delta_p \qquad (7)$$

where irms indicates an ideal root-mean-square, and the matrices and vectors are defined by partitioning Eq. 5, as shown below:

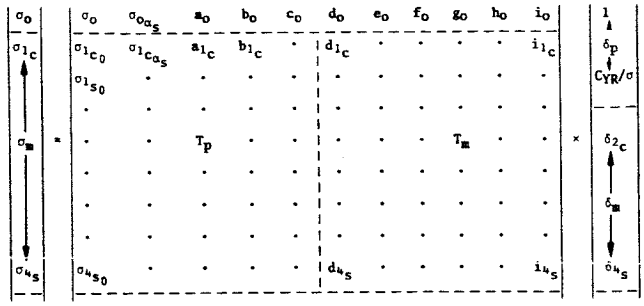

These ideal vectors have also been calculated for the 30 cases with resultant rms reductions between 40 and 66%. Figure 5 shows a few of these cases, with stress calculated for "zero" multicyclic. These stresses have been, in effect, extrapolated, whereas the data in Figure 2 were measured. As indicated on the figure, the ideal rms control also reduced peak-to-peak stresses. For the 30 cases investigated, the ideal rms control vectors reduced peak-to-peak stresses from 39 to 65%.

The ideal multicyclic vectors given by Eq. 7 are a function of the flight condition as defined by shaft axis inclination, advance ratio, and the rotor's lift, propulsive, and side-force coefficients. The elements of these ideal rms control vectors have been plotted against propulsive force coefficient in Figure 6. Different symbols denote the corresponding lift coefficient levels. The effects of C_{LR}/σ and C_{XR}/σ and shaft axis inclination are quite apparent. (The range of side-force coefficients was insufficient to deduce its effect.) The third and fourth harmonics were quite constant in phase; hence, only their amplitudes have been plotted. Note that these harmonics do not appear sensitive to rotor lift coefficient.

Transmitted Vibration Forces

The rotor suspension system for the wind tunnel tests incorporated a six-component balance and a parallelogram support discussed in References 4 and 5. The parallelogram support absorbed inplane vibratory loads very effectively, so that the vertical vibratory loads were the only ones of interest. These loads are due to thrustwise hub shears in combination with the motions of the hub due to the parallelogram support. For this two-bladed rotor, the transmitted loads contained only even-order harmonics as shown in Figure 3. These loads may also be related to the harmonics of the jet-flap deflection by a transfer matrix, as shown by Eq. 8.

With this transfer matrix it is possible to eliminate the second and fourth harmonics of the vertical vibratory loads by the same procedures used to eliminate the higher harmonic blade-bending stresses if two of the harmonic components of the control vector are specified. The resulting

$$\begin{vmatrix} V_o \\ V_{2_c} \\ V_{2_s} \\ V_{4_c} \\ V_{4_s} \end{vmatrix} = \begin{vmatrix} V_{o_0} & V_{o_{\alpha_s}} & p_o & q_o & r_o & \cdot & \cdot & \cdot \\ V_{2_{c_0}} & V_{2_{c_{\alpha_s}}} & p_{2_c} & q_{2_c} & r_{2_c} & \cdot & \cdot & \cdot \\ \cdot & \cdot & \cdot & \cdot & \cdot & \cdot & \cdot & \cdot \\ \cdot & \cdot & \cdot & \cdot & \cdot & \cdot & \cdot & \cdot \\ \cdot & \cdot & \cdot & \cdot & \cdot & \cdot & \cdot & \cdot \end{vmatrix} \times \begin{vmatrix} 1 \\ \alpha_s \\ C_{LR}/\sigma \\ C_{XR}/\sigma \\ C_{YR}/\sigma \\ \delta_{2_c} \\ \delta_{2_s} \\ \delta_{3_c} \\ \delta_{3_s} \\ \delta_{4_c} \\ \delta_{4_s} \end{vmatrix} \quad (8)$$

$$\begin{vmatrix} V_{2_c} \\ V_{2_s} \\ V_{4_c} \\ V_{4_s} \\ \sigma_{3_s} \\ \sigma_{4_s} \end{vmatrix} = \begin{vmatrix} V_{2_{c_0}} & V_{2_{c_{\alpha_s}}} & p_{2_c} & q_{2_c} & r_{2_c} & \cdot & \cdot & \cdot \\ V_{2_{s_0}} & V_{2_{s_{\alpha_s}}} & p_{2_s} & \cdot & \cdot & \cdot & \cdot & \cdot \\ V_{4_{c_0}} & V_{4_{c_{\alpha_s}}} & p_{4_c} & \cdot & \cdot & \cdot & \cdot & \cdot \\ V_{4_{s_0}} & V_{4_{s_{\alpha_s}}} & p_{4_s} & \cdot & \cdot & \cdot & \cdot & \cdot \\ \sigma_{3_{s_0}} & \sigma_{3_{s_{\alpha_s}}} & a_{3_s} & b_{3_s} & c_{3_s} & \cdot & \cdot & \cdot \\ \sigma_{4_{s_0}} & \sigma_{4_{s_{\alpha_s}}} & a_{4_s} & \cdot & \cdot & \cdot & \cdot & \cdot \end{vmatrix} \times \begin{vmatrix} 1 \\ \alpha_s \\ C_{LR}/\sigma \\ C_{XR}/\sigma \\ C_{YR}/\sigma \\ \delta_{2_c} \\ \delta_{2_s} \\ \delta_{3_c} \\ \delta_{3_s} \\ \delta_{4_c} \\ \delta_{4_s} \end{vmatrix} \quad (9)$$

where

$$V_{n_c} \triangleq (F_1 + F_2 + F_3)_{n_c}$$

$$V_{n_s} \triangleq (F_1 + F_2 + F_3)_{n_s}$$

deflection harmonic components would define ideal vibration control vectors whose elements would depend also on the flight condition. Such vectors have been calculated for the third harmonic jet-flap deflections set to zero and are shown in Reference 6. These vectors (calculated for 12 cases) show the second and fourth control components to be constant in phase, but they are significantly different in phase and magnitude from the ideal stress control vectors. As might be expected, the lack of third harmonic jet-flap deflection, and a large fourth harmonic requirement, resulted in very large third harmonic blade stresses, when these ideal vibration control vectors were input into Eq. 5.

When ideal rms (stress) control vectors are input into Eq. 8, the vibratory loads sometime increase. A sample case is shown in Figure 7. Shown are the stress and vibratory loads for "zero" multicyclic, the actual multicyclic used in the wind tunnel test, and the ideal rms control vector. The actual peak-to-peak stress reduction is 39% and the ideal stress reduction is 47%. The ideal rms control vector increased the vibratory loads 78%, while the actual control increased them by only 48%. The upper portion of the figure shows the actual and ideal multicyclic component amplitudes and phases. The actual phases are quite close to the ideal phases, but the actual third and fourth harmonics are too low. It is also apparent, however, that these third and fourth harmonics caused the increase in vibratory loads.

It is apparent from the foregoing that some sort of combined matrix is needed to effect reductions in both stress and vibratory loads. It would not be possible to eliminate all of the harmonic components since for this test rotor, we only have six elements in the control vector, δ_{2_c}, δ_{2_s} through δ_{4_s}. It is possible, however, to eliminate six of the response elements. For example, one may select both harmonics of vibratory loads and the third and fourth sine components of stress — the largest of the stress components — and construct a transfer matrix such as shown below. The multicyclic deflections required are determined by the solution of this equation for the condition that V_{2_c}, V_{2_s}, V_{4_c}, V_{4_s}, σ_{3_s} and σ_{4_s} are all equal to zero. The remainder of the stress coefficients and V_0 can be determined from Eqs. 5 and 8 after the multicyclic control vector has been evaluated.

Of course, other ideal control vectors are also possible, and these would depend quite obviously on the particular rotor and flap control system and the number of blades, etc. The blades' natural frequencies, the position and extent of the flaps will all affect the blade stress transfer matrix. The number of blades will have a definite effect on the harmonics of blade loads transmitted to the nonrotating system; hence, the compromise between loads and stress control would differ in each case. However, the basic method for analysis used herein can be applied to any such investigation, experimental or theoretical.

Multicyclic Lift Requirements

The results presented here correspond to a specific jet-flap driven rotor. The question arises to what extent other circulation control means would permit a similar reduction of stress levels in the blades and of vibratory loads. Such systems as mechanical flaps, servo flaps controlling the twist of the blades, low-powered jet-flaps, conventional rotor blades having multicyclic control in addition to swash-plate control may introduce multicyclic lift effects and are, at least conceptually, capable of producing some amount of stress and vibration alleviation. This capability being assumed, the problem then becomes one of degree rather than one of nature. The systems differ only by their unsteady flow characteristics but have to offer the similar capability of producing high frequency lift inputs up to at least the fourth harmonic of rotor frequency. The remaining question is "How much incremental lift is needed?"

There was no instrumentation on the blades to determine the local lift variations, and had there been, it would not be possible to determine the amount due to the multicyclic jet-flap deflection directly. However, knowing the jet-flap deflection and the average jet momentum coefficient, it is possible to calculate an incremental lift coefficient, assuming a nonvariant alpha. This has been done for several of the wind tunnel test cases and the Δc_l ranged from ±0.12 to ±0.68 for the higher harmonic components. Figure 8 shows the variation of the local blade element coefficient Δc_l for an ideal rms control vector. The corresponding stress reduction projected for this case would be 50%. (Note that Δc_l is approximately ±0.68.) The figur shows that the highest lift variation occurs on the retreating blade, a fact that proves favorable for the jet-flap, whose capability increases in low Mach-number flows.

It is believed that these magnitudes of Δc_l are obtainable with low powered jet-flaps. Assuming that somewhat lesser incremental lift variations would be necessary for softer conventional rotor blades, multicyclic mechanical and/or servo-flap control appears feasible. Two study contracts underway also support this contention.

The sensitivity of the blade stresses and vibration to multicyclic control and our present inability to predict harmonic loading, stresses, and and vibration, leads to the desirability of completely automating multicyclic control such as would be attained by feedback control systems. The Giravions Dorand firm is engaged in a basic research program to develop such a feedback system and early results are quite encouraging.

CONCLUDING REMARKS

Wind tunnel tests of a jet-flap rotor simulating forward flight have shown that it is possible to modulate the rotor's loading by means of a multicyclic control system so that rotor blade stresses and vibratory loads transmitted to the fuselage can be reduced. A method of analyzing the multivariable problem has been presented and several "ideal" control schedules are presented. The schedules themselves are applicable only to the specific jet-flap rotor tested, but the method of determining the schedules is applicable to similar systems. It was shown that it is not possible to eliminate all oscillatory blade-bending and vibratory loads with a system such as the test rotor, which had only three higher harmonics of azimuthal control. Such limited systems can, however, be used to eliminate specific selected harmonic component stress and vibration responses.

A simplified estimate of the incremental lift coefficient being generated multicyclically by the test rotor indicates that similar multicyclic mechanical or low-powered jet-flaps could also be sucessful in reducing blade stresses or vibratory loads.

References

1. Aronson, R. B. and Jines, R. H., "Helicopter Development Reliability Test Requirements, Vol. I - Study Results," USAAMRDL TR 71-18A, February 1972.

2. Veca, A. C., "Vibration Effects on Helicopter Reliability and Maintainability," USAAMRDL TR 73-11, April 1973.

3. Evans, William T. and McCloud, John L., III, "An Analytical Investigation of a Rotor Driven and Controlled by a Jet-Flap," NASA TN D-3028.

4. McCloud, John L., III, Evans, William T., and Biggers, James C., "Performance Characteristics of a Jet-Flap Rotor," in Conference on V/STOL and STOL Aircraft, Ames Research Center, NASA SP-116, 1966, pp. 29-40.

5. McCloud, John L., III, "Studies of a Large-Scale Jet-Flap Rotor in the 40- by 80-Foot Wind Tunnel," presented at Mideast Region Symposium A.H.S. Status of Testing and Modeling Techniques for V/STOL Aircraft, Philadelphia, PA, October 1972.

6. Kretz, M., Aubrun, J.-N., Larche, M., "March 1971 Wind-Tunnel Tests of the Dorand DH 2011 Jet-Flap Rotor" NASA CRs 114693 and 114694.

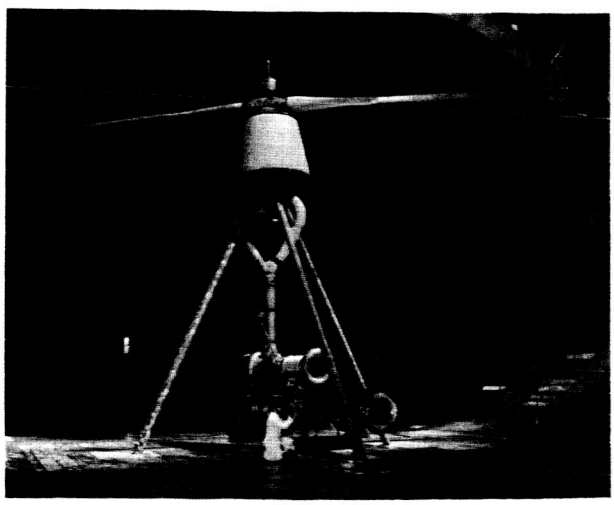

Figure 1. Jet-flap rotor in the Ames 40- by 80-Foot Wind Tunnel.

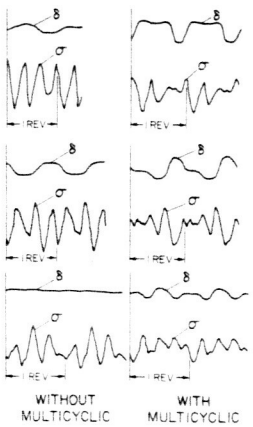

Figure 2. Effect of multicyclic jet-flap deflection on blade stresses.

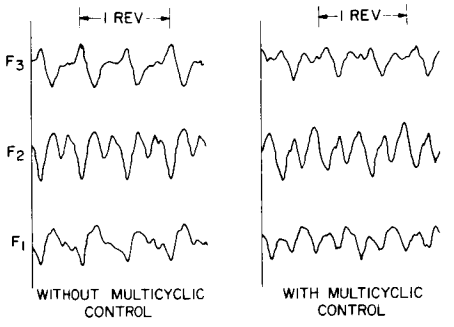

Figure 3. Effect of multicyclic jet-flap deflection on vertical forces below hub.

σ_0	268	-23	3	-1	1	0	1	1	2	-5	3	1
σ_{1_c}	49	3	1	2	-11	0	5	-2	6	10	1	α_s
σ_{1_s}	-441	-36	2	-14	2	0	-3	0	-2	-13	7	C_{LR}/σ
σ_{2_c}	287	-19	-2	9	-1	12	4	-4	2	6	0	C_{XR}/σ
σ_{2_s} =	12	2	0	1	-5	0	14	-2	1	10	-3	C_{YR}/σ × δ_{2_c}
σ_{3_c}	-230	-12	4	-11	-15	-5	-13	32	-20	-18	18	δ_{2_s}
σ_{3_s}	-409	-18	2	-7	-17	10	6	-15	50	-52	32	δ_{3_c}
σ_{4_c}	660	42	-6	21	27	11	-5	18	27	-21	-20	δ_{3_s}
σ_{4_s}	75	1	0	5	3	0	7	-7	5	59	-78	δ_{4_c}
												δ_{4_s}

σ_{45} RADIAL STATION
30 CASES AT $V/\Omega R = .4$

Figure 4. Transfer matrix for fixed flight conditions.

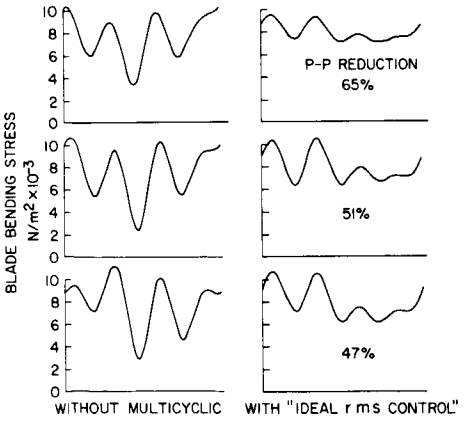

Figure 5. Calculated blade bending stresses using equations 5, 6, and 7.

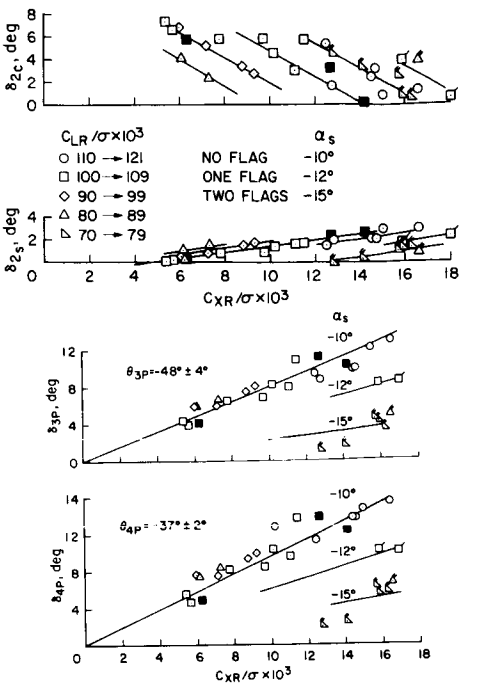

Figure 6. Ideal rms vector relations.

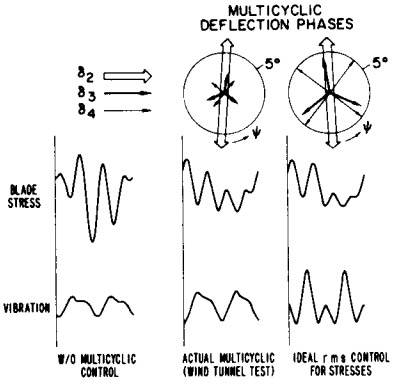

Figure 7. Calculated blade stresses and vibratory loads using equations 5, 6, 7 and 8.

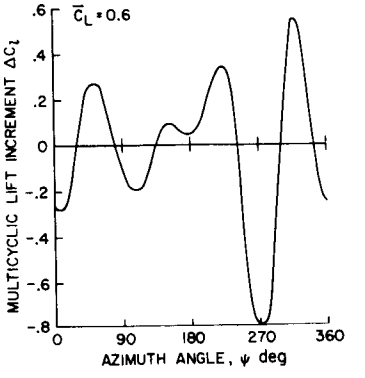

Figure 8. Variation of the estimated increment of blade section lift coefficient due to multicyclic jet-flap deflection.